

# Four-tori solution in a magnetohydrodynamic Couette flow as a consequence of azimuthal symmetry breaking

F. Garcia,<sup>1</sup> M. Seilmayer,<sup>1</sup> A. Giesecke,<sup>1</sup> and F. Stefani<sup>1</sup>

<sup>1</sup>*Department of Magnetohydrodynamics, Helmholtz-Zentrum Dresden-Rossendorf, Bautzner Landstraße 400, D-01328 Dresden, Germany*

(Dated: July 8, 2020)

The occurrence of four-tori in differentially rotating magnetohydrodynamic (MHD) flows in spherical geometry is understood in terms of a sequence of Hopf bifurcations breaking the azimuthal symmetry of the flow as the applied magnetic field strength is varied. These flows originate from unstable rotating waves (RW), and two-tori modulated rotating waves (MRW), with broken equatorial symmetry but having azimuthal symmetry  $m = 4$ . A posterior bifurcation gives rise to  $m = 2$  symmetric three-tori MRW and a further bifurcation to a four-tori MRW which has lost all the spatial symmetries. This bifurcation scenario may be favoured when differential rotation is increased and rotating waves with azimuthal symmetry  $m$ , product of several prime numbers, emerge at sufficiently large magnetic field.

PACS numbers:

Understanding how systems become chaotic is of fundamental importance in many applications. Biological systems [1, 2], financial models [3], road traffic modelling [4], laser physics [5], neural networks [6], and simulations in fluid dynamics [7], or magnetohydrodynamics [8], exhibit transitions from regular oscillatory behaviour to a chaotic regime. Quite often, this transition follows the Newhouse-Ruelle-Takens (NRT) [9] scenario in which after a few bifurcations, involving quasiperiodic states, chaos emerges. According to the NRT theorem quasiperiodic oscillatory motions with 3 or more fundamental frequencies, i. e. three or higher dimensional tori, are unstable to small perturbations and thus unlikely to occur. However, the numerical experiments of [10] first evidenced that the mathematical notion of small perturbations is a key issue and that in case of an appropriate spatial structure of the perturbations a three-tori solution may well be observed in real nonlinear systems. Since then, the existence of three-tori has been confirmed in experiments on electronic circuits [11, 12], solid mechanics [13], hydrodynamics [14], Rayleigh-Bénard convection [15] and magnetohydrodynamics (MHD) [16]. The study of MHD flows is indeed of fundamental relevance in geophysics and astrophysics which motivated experiments [17, 18] and simulations [19, 20] that investigate for example the role of chaotic and/or turbulent flows for planetary and stellar dynamos [21], or the turbulent transport processes occurring in accretion disks [22] where the magnetorotational instability (MRI) [23] plays a fundamental role.

Symmetries in physical systems provide a way to circumvent the NRT theorem because the bifurcations occurring in these systems may be nongeneric. Their understanding is of relevance as the character of an underlying symmetry group in general is reflected in the possible solutions and their evolution in time, e.g. in terms of conservation laws. This is especially the case in fluid dynam-

ics [24], or magnetohydrodynamics, where the appearance of three-tori solutions has been interpreted as a consequence of bifurcations [16, 25], which may introduce a breaking of symmetry [8, 26, 27]. Quasiperiodic tori with more than three frequencies are however rarely found in systems with moderate and large number of degrees of freedom (e.g. [6]). For instance, the existence of four-tori solutions has been attributed to the nongeneric character of two-dimensional Rayleigh-Bénard convection [28], or to spatial localisation of weakly coupled individual modes in [15, 29]. The latter studies pointed out the relevance of the spatial structure of the solutions for the emergence of chaos in large-scale systems.

In this Letter we investigate the emergence of four-tori and chaotic flows in simulations of a magnetised spherical Couette (MSC) system. Using an accurate frequency analysis (based on Laskar's algorithm [30]) and Poincaré sections, we find that consecutive symmetry breakings caused by various Hopf bifurcations determine the evolution of the system and accompany the route to chaotic behaviour. The MSC system constitutes a paradigmatic MHD problem [31–34] that is of relevance for differentially rotating, electrically conducting flows. Flows driven by differential rotation, which have been investigated in several experiments [35–40], govern the dynamics in the interior of stars and/or planets [20] where they constitute a possible source for MHD wave phenomena [41], dynamo action [59], and perhaps even for the generation of gravitational wave signals from neutron stars [42, 43].

In terms of symmetry theory [44] the MSC problem is a  $\mathbf{SO}(2) \times \mathbf{Z}_2$  equivariant system, i. e., invariant by azimuthal rotations ( $\mathbf{SO}(2)$ ) and reflections with respect to the equatorial plane ( $\mathbf{Z}_2$ ). In  $\mathbf{SO}(2)$  symmetric systems, branches of rotating waves (RWs), either stable or unstable, appear after the axisymmetric base state becomes unstable (primary Hopf bifurcations [24]). Succes-

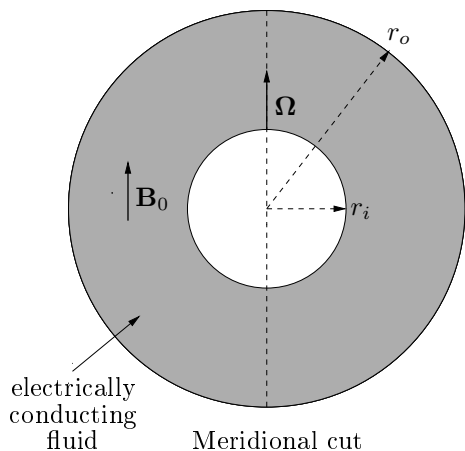


FIG. 1: Scheme of the magnetized spherical Couette (MSC) geometry.

sive Hopf bifurcations [45, 46] give rise to quasiperiodic modulated rotating waves (MRWs) and to chaotic turbulent flows, usually following the NRT scenario [45]. In the particular case of the MSC, when the magnetic field is varied, branches of RWs with a  $m$ -fold azimuthal symmetry with a prime number  $m = 2, 3$  [32, 47] give rise to stable two- and three-tori MRWs [48], and eventually chaotic flows [8], though four-tori MRWs have not yet been found. In the following, we show that MHD four-tori solutions in terms of MRWs can be obtained after successive azimuthal symmetry breaking Hopf bifurcations from a parent branch of RW having  $m$ -fold symmetry which is not a prime number, in this case  $m = 4$ . Note that when  $m$  is a prime number only one symmetry breaking bifurcation can take place as the flows are equatorially asymmetric so that the case  $m = 4$  constitutes the lowest non-trivial possibility for azimuthal symmetry breaking with multiple bifurcations.

We consider an electrically conducting fluid of density  $\rho$ , kinematic viscosity  $\nu$ , magnetic diffusivity  $\eta = 1/(\sigma\mu_0)$  (where  $\mu_0$  is the magnetic permeability of the free-space and  $\sigma$  is the electrical conductivity). The fluid is bounded by two spheres with radius  $r_i$  and  $r_o$ , respectively, with the outer sphere being at rest and the inner sphere rotating at angular velocity  $\Omega$  around the vertical axis  $\hat{\mathbf{e}}_z$ . A uniform axial magnetic field of amplitude  $B_0$  is imposed as in the HEDGEHOG experiment [38] (see Fig 1). Scaling the length, time, velocity and magnetic field with  $d = r_o - r_i$ ,  $d^2/\nu$ ,  $r_i\Omega$  and  $B_0$ , respectively, the temporal evolution of the system is governed by the Navier-Stokes equation and the induction equation which read:

$$\begin{aligned} \partial_t \mathbf{v} + \text{Re}(\mathbf{v} \cdot \nabla) \mathbf{v} &= -\nabla p + \nabla^2 \mathbf{v} + \text{Ha}^2 (\nabla \times \mathbf{b}) \times \hat{\mathbf{e}}_z, \\ 0 &= \nabla \times (\mathbf{v} \times \hat{\mathbf{e}}_z) + \nabla^2 \mathbf{b}, \quad \nabla \cdot \mathbf{v} = 0, \quad \nabla \cdot \mathbf{b} = 0, \end{aligned}$$

where  $\text{Re} = \frac{\Omega r_i d}{\nu}$  is the Reynolds number,  $\text{Ha} = B_0 d (\frac{\sigma}{\rho\nu})^{1/2}$  is the Hartmann number,  $\mathbf{v}$  the velocity field

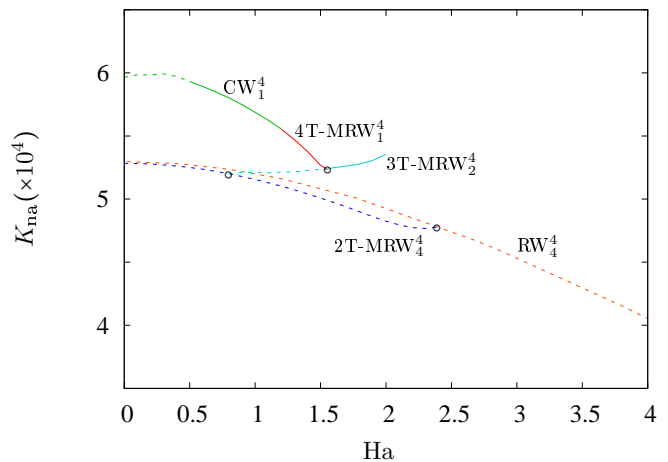


FIG. 2: Bifurcation diagram of the volume-averaged non-axisymmetric kinetic energy density  $K_{\text{na}}$  versus  $\text{Ha}$ . Solid (dashed) lines are used for stable (unstable) flows. Branches of rotating waves  $\text{RW}_m^{m_{\text{max}}}$ , modulated rotating waves  $\text{MRW}_m^{m_{\text{max}}}$ , and chaotic waves  $\text{CW}_m^{m_{\text{max}}}$  are shown. MRWs with 2, 3 and 4 frequencies are labelled as 2T, 3T and 4T, respectively. The colors distinguish the various solutions according to the corresponding label.

and  $\mathbf{b}$  the deviation of magnetic field from the axial applied field. Here we use the inductionless approximation which is valid in the limit of small magnetic Reynolds number,  $\text{Rm} = \Omega r_i d / \eta \ll 1$ . This condition is well met when considering the liquid metal GaInSn, with magnetic Prandtl number  $\text{Pm} = \nu / \eta \sim O(10^{-6})$  [49], at moderate  $\text{Re} = 10^3$  (as used in the experiment [38]) since  $\text{Rm} = \text{PmRe} \sim 10^{-3}$ . The aspect ratio is  $\chi = r_i / r_o = 0.5$  and no-slip ( $v_r = v_\theta = v_\varphi = 0$ ) at  $r = r_o$  and constant rotation ( $v_r = v_\theta = 0$ ,  $v_\varphi = \sin \theta$ ) at  $r = r_i$  are the boundary conditions imposed on the velocity field. For the magnetic field, insulating boundary conditions are considered in accordance with typical experimental setups [35]. Spectral methods –spherical harmonics in the angular coordinates– and a collocation method in the radial direction– and high order implicit-explicit backward-differentiation (IMEX–BDF) time schemes are employed for solving the MSC equations (see [8, 47] for details).

The solutions are classified according to their azimuthal symmetry  $m$ , the wave number with the largest volume-averaged kinetic energy  $m_{\text{max}}$ , and their type of time dependence. In this way, branches of RWs and MRWs are labelled as  $\text{RW}_m^{m_{\text{max}}}$  and  $\text{MRW}_m^{m_{\text{max}}}$ . The latter can be quasiperiodic with 2, 3 and 4 frequencies and are labelled as 2T, 3T and 4T, respectively. The branches of equatorially asymmetric  $\text{RW}_2^2$ ,  $\text{RW}_3^3$ , and  $\text{RW}_4^4$  which bifurcate from the base state at  $\text{Ha} = 12.2$  [32] were computed in [47] by means of continuation methods [50–52]. The present study focuses on the analysis of the MRW bifurcating from the unstable branch  $\text{RW}_4^4$  for small  $\text{Ha} < 2.5$  at fixed  $\text{Re} = 10^3$ . These MRWs have been obtained by means of direct numerical simulations

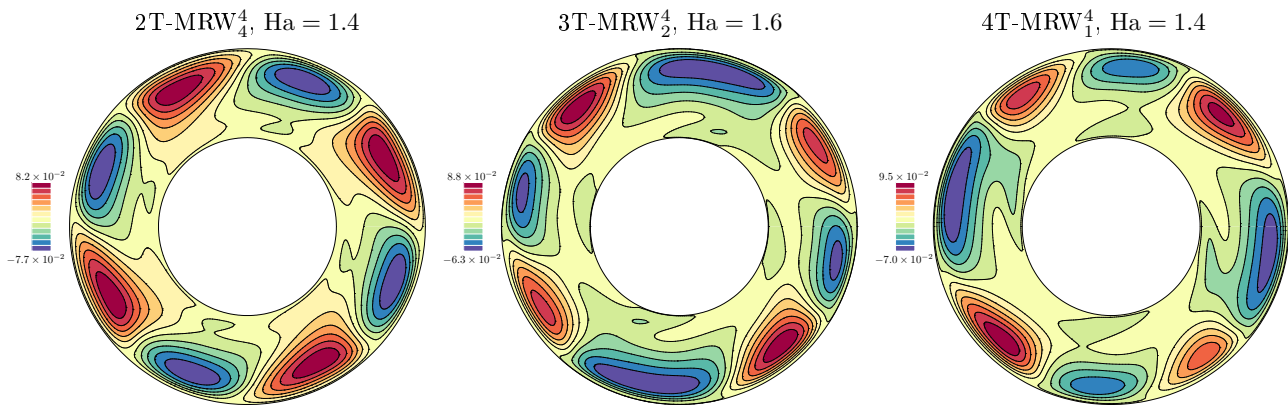


FIG. 3: Contour plots of the nonaxisymmetric component of the radial velocity on a colatitudinal section at  $\theta \approx 93$ . The azimuthal symmetry is broken from left to right: from  $m = 4$  to  $m = 2$  and from  $m = 2$  to  $m = 1$ .

(DNS) of the MSC equations with  $n_r = 40$  radial collocation points and a spherical harmonic truncation parameter of  $L_{\max} = 84$ . The dimension of the system is then  $n = (2L_{\max}^2 + 4L_{\max})(n_r - 1) = 563472$ . The results for an example of four-tori at  $\text{Ha} = 1.4$  are confirmed for increased resolution with  $n_r = 60$  and  $L_{\max} = 126$ . The time and volume-averaged nonaxisymmetric kinetic energy density  $K_{\text{na}}$  is employed as a proxy for the study of time dependent flows because they initially bifurcate from the base state which is axisymmetric (only the  $m = 0$  mode is nonzero in the spherical harmonics expansion).

The bifurcation diagram in Fig. 2 displays  $K_{\text{na}}$  versus  $\text{Ha}$  and the bifurcation points are marked with circles. By decreasing  $\text{Ha}$ , periodic  $\text{RW}_4^4$  undergo a Hopf bifurcation to 2T  $\text{MRW}_4^4$  around  $\text{Ha} \approx 2.4$  which then extends down to  $\text{Ha} = 0$ . These flows are obtained with time integrations with the azimuthal symmetry constrained to  $m = 4$  and are unstable to small random perturbations with azimuthal symmetry  $m = 1$ . Another branch of unstable solutions appears at  $\text{Ha} = 0.8$  via a secondary subcritical Hopf bifurcation on the 2T  $\text{MRW}_4^4$  (blue dashed curve) branch which breaks the  $m = 4$  symmetry to  $m = 2$  and finally leads to the emergence of an unstable 3T  $\text{MRW}_2^4$  branch (light blue dashed curve). The latter extends for increasing  $\text{Ha}$  and becomes stable at  $\text{Ha} \approx 1.52$  where a branch of 4T  $\text{MRW}_1^4$  is born thanks to a tertiary subcritical Hopf bifurcation breaking the  $m = 2$  symmetry (red curve). This branch becomes chaotic for  $\text{Ha} \lesssim 1.25$  (green curve). The contour plots of the  $m \neq 0$  component of the radial velocity, on a colatitudinal section slightly below the equatorial plane, are displayed in Fig. 3 for one example of each type of MRW with azimuthal symmetry  $m = 4, m = 2$ , and  $m = 1$  (from left to right).

The time dependence of RWs is described by a uniform azimuthal rotation of a fixed flow pattern whereas for MRWs the pattern is azimuthally rotating but modulated with additional frequencies (e.g. [45]). Thus, a frequency analysis of any azimuthally averaged property provides

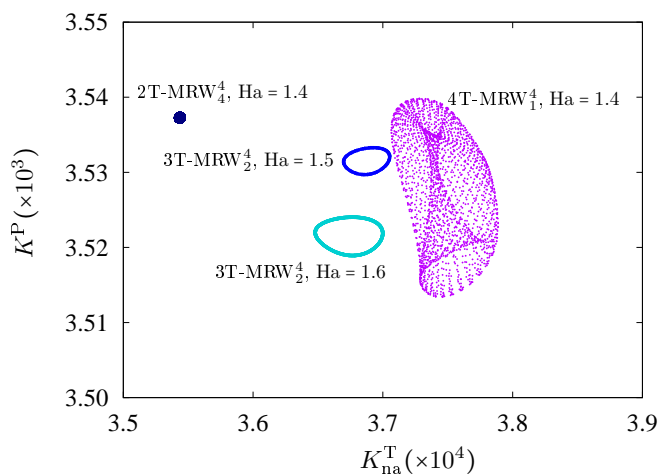


FIG. 4: Poincaré sections defined by the constraint  $K(t) = \bar{K}$ ,  $K$  being the volume-averaged kinetic energy and  $\bar{K}$  its time average. The volume-averaged poloidal kinetic energy  $K^{\text{P}}$  is displayed versus the volume-averaged toroidal nonaxisymmetric energy  $K_{\text{na}}^{\text{T}}$ . Because volume-averaged properties are considered, the Poincaré sections of 2T, 3T and 4T are a single point, a closed curve and a band of dots, respectively.

one frequency less than the analysis of a localised particular flow component. Because of this, Poincaré sections defined by the constraint  $K(t) = \bar{K}$ ,  $K$  being the volume-averaged kinetic energy and  $\bar{K}$  its time average, appear as a single point for 2T, a closed curve for 3T and a band of points for 4T (see Fig. 4). To confirm the regular behavior of 2T, 3T, and 4T MRWs we perform a frequency analysis. The frequencies giving rise to the modulation are accurately determined from the time series of  $K_4$  ( $K$  restricted to the  $m = 4$  mode) by means of a FFT-based optimisation algorithm [30]. If the solution is regular the frequencies do not depend (within the frequency determination accuracy) on the particular time window used for the analysis [53, 54]. Sufficiently wide time windows (5 – 40 time units) over large time series

(100 time units) are considered which leads to a relative accuracy around  $10^{-5}$ . For  $\text{Ha} \lesssim 1.25$  the variation of the main frequency  $f_1$  is larger than the accuracy and thus 4T  $\text{MRW}_1^4$  become chaotic. Frequency spectra are displayed in Fig. 5(a,b) for the same MRW as shown in Fig. 3 and in Fig. 5(c) for a chaotic wave. One fundamental frequency  $f_1$  and its multiples are present in the spectrum of the 2T  $\text{MRW}_4^4$  whereas a second frequency  $f_2$  and few combinations  $k_1 f_1 + k_2 f_2$ , with integer  $k_i$ , are present for the 3T  $\text{MRW}_2^4$  (Fig. 5(a)). In contrast, the spectrum of 4T  $\text{MRW}_1^4$  exhibits several combinations  $k_1 f_1 + k_2 f_2 + k_3 f_3$  revealing a complex time dependence. We have checked that  $\epsilon_r = |f - k_1 f_1 - k_2 f_2 - k_3 f_3|/f < 10^{-5}$  for all of the 76 frequencies obtained in Fig. 5(b) and  $-6 \leq k_i \leq 6$ . This is not true in the case of the chaotic wave as the frequencies depend on time and thus on the particular time window used for the analyses (Fig. 5(c)). Nevertheless, the main frequencies of  $\text{MRW}_1^4$  generating the chaotic flow can still be identified.

The present study evidences for the first time that four-tori solutions are physically possible in MHD problems and can be explained in terms of bifurcation theory. The bifurcation scenario resembles the NRT scenario but involves two additional Hopf bifurcations, including a sub-critical bifurcation leading to a stabilisation of a three-tori solution. This kind of stabilisation was also found in [55], but for axisymmetric steady states, in the case of purely hydrodynamic spherical Couette (SC) flows. Further SC experiments [56] are in accordance with the NRT scenario, but only two-tori were detected before the regime of chaotic flows. Similarly, three or four-tori have not been found in a comprehensive study of the different flow regimes in the SC system with positive or negative differential rotation [34]. When the magnetic field is included, several MSC regimes have been studied recently [31, 39, 57] but the existence of quasiperiodic flows with three frequencies has not been shown until [8].

The fundamental result presented here is that in a system with symmetry, more symmetry breaking bifurcations may be required in the NRT scenario until a flow can become chaotic, and thus regular motions with more than three frequencies are likely to occur. The additional frequency the system acquires at the bifurcation is usually smaller than the previous fundamental one (Fig. 5) and thus capturing the several frequencies of quasiperiodic attractors may require rather long time evolutions of the system. This is a key issue for experiments [38] which would involve hours (or even days) of measurements in case of typical laboratory setup. The results also bear relevance for the MRI as previous experiments [35] may be understood in terms of MSC instabilities [31, 57], as those analysed here.

F. G. was supported by the Alexander von Humboldt Foundation. This project has also received funding from the European Research Council (ERC) under the European Unions Horizon 2020 research and innovation pro-

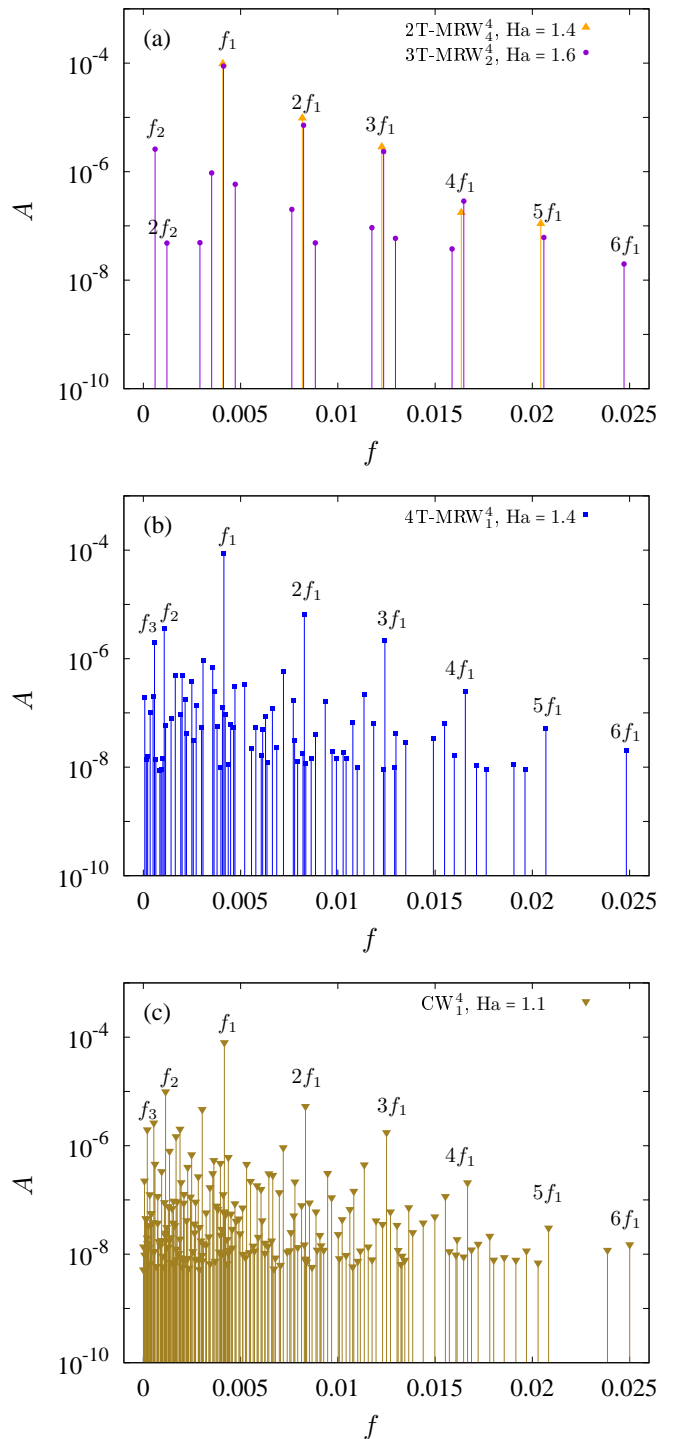


FIG. 5: Frequency analysis of the time series of the volume-averaged kinetic energy density  $K_4$  of the  $m = 4$  mode for (a) 3T- $\text{MRW}_2^4$  at  $\text{Ha} = 1.6$  and (b) 4T- $\text{MRW}_1^4$  at  $\text{Ha} = 1.4$ . (c) Chaotic flow  $\text{CW}_1^4$  at  $\text{Ha} = 1.1$ . The volume-average removes one fundamental frequency of the flow associated to its azimuthal drift.

gramme (grant agreement No 787544).

- 
- [1] G. B. Ermentrout, *J. Math. Biol.* **23**, 55 (1985).
- [2] M. G. Grigorov, *Bioinformatics* **22**, 1424 (2006).
- [3] H.-W. Lorenz, *J. Econ. Behav. Organ.* **8**, 397 (1987).
- [4] L. A. Safonov, E. Tomer, V. V. Strygin, Y. Ashkenazy, and S. Havlin, *CHAOS* **12**, 1006 (2002).
- [5] O. Hess, D. Merbach, H.-P. Herzog, and E. Scholl, *Phys. Lett. A* **194**, 289 (1994).
- [6] D. Albers and J. Sprott, *Physica D* **223**, 194 (2006).
- [7] D. Castaño, M. C. Navarro, and H. Herrero, *Phys. Rev. E* **93**, 013117 (2016).
- [8] F. Garcia, M. Seilmayer, A. Giesecke, and F. Stefani, *CHAOS* (2020).
- [9] S. Newhouse, D. Ruelle, and F. Takens, *Commun. Math. Phys.* **64**, 35 (1978).
- [10] C. Grebogi, E. Ott, and J. A. Yorke, *Phys. Rev. Lett.* **51**, 339 (1983).
- [11] A. Cumming and P. S. Linsay, *Phys. Rev. Lett.* **60**, 2719 (1988).
- [12] E. Sánchez, D. Pazó, and M. A. Matías, *CHAOS* **16**, 033122 (2006).
- [13] R. Alaggio and G. Rega, *Physica D* **137**, 70 (2000).
- [14] J. Langenberg, G. Pfister, and J. Abshagen, *Phys. Rev. E* **70**, 046209 (2004).
- [15] R. W. Walden, P. Kolodner, A. Passner, and C. M. Surko, *Phys. Rev. Lett.* **53**, 242 (1984).
- [16] A. Libchaber, S. Fauvé, and C. Laroche, *Physica D* **7**, 73 (1983).
- [17] F. Stefani, T. Gundrum, G. Gerbeth, G. Rüdiger, M. Schultz, J. Szklarski, and R. Hollerbach, *Phys. Rev. Lett.* **97**, 184502 (2006).
- [18] A. Gailitis, O. Lielausis, E. Platacis, G. Gerbeth, and F. Stefani, *Rev. Modern Phys.* **74**, 973 (2002).
- [19] P. H. Roberts and G. A. Glatzmaier, *Rev. Modern Phys.* **72**, 1081 (2000).
- [20] C. A. Jones, *Ann. Rev. Fluid Mech.* **43**, 583 (2011).
- [21] P. H. Roberts and M. Stix, *NCAR Technical Notes Collection TN-60+IA* (1971).
- [22] S. A. Balbus and J. F. Hawley, *Rev. Modern Phys.* **70**, 1 (1998).
- [23] S. A. Balbus and J. F. Hawley, *Astrophys. J.* **376**, 214 (1991).
- [24] J. D. Crawford and E. Knobloch, *Ann. Rev. Fluid Mech.* **23**, 341 (1991).
- [25] J. M. Lopez and F. Marques, *Phys. Rev. Lett.* **85**, 972 (2000).
- [26] S. Altmeyer, Y. Do, F. Marques, and J. M. Lopez, *Phys. Rev. E* **86**, 046316 (2012).
- [27] F. Garcia, M. Net, and J. Sánchez, *Phys. Rev. E* **93**, 013119 (2016).
- [28] E. Zienicke, N. Seehafer, and F. Feudel, *Phys. Rev. E* **57**, 428 (1998).
- [29] K. He, *Phys. Rev. Lett.* **94**, 034101 (2005).
- [30] J. Laskar, *Celestial Mech. Dyn. Astr.* **56**, 191 (1993).
- [31] R. Hollerbach, *Proc. Roy. Soc. Lond. A* **465**, 2003 (2009).
- [32] V. Travníkov, K. Eckert, and S. Odenbach, *Acta Mech.* **219**, 255 (2011).
- [33] A. Figueroa, N. Schaeffer, H.-C. Nataf, and D. Schmitt, *J. Fluid Mech.* **716**, 445 (2013).
- [34] J. Wicht, *J. Fluid Mech.* **738**, 184 (2014).
- [35] D. R. Sisan, N. Mujica, W. A. Tillotson, Y. M. Huang, W. Dorland, A. B. Hassam, T. M. Antonsen, and D. P. Lathrop, *Phys. Rev. Lett.* **93**, 114502 (2004).
- [36] D. S. Zimmerman, S. A. Triana, and D. P. Lathrop, *Phys. Fluids* **23**, 065104 (2011).
- [37] M. Hoff, U. Harlander, and C. Egbers, *J. Fluid Mech.* **789**, 589616 (2016).
- [38] C. Kasprzyk, E. Kaplan, M. Seilmayer, and F. Stefani, *Magnetohydrodynamics* **53**, 393 (2017).
- [39] E. J. Kaplan, H.-C. Nataf, and N. Schaeffer, *Phys. Rev. Fluids* **3**, 034608 (2018).
- [40] A. Barik, S. A. Triana, M. Hoff, and J. Wicht, *J. Fluid Mech.* **843**, 211 (2018).
- [41] H. C. Spruit, *Astron. & Astrophys.* **381**, 923 (2002).
- [42] C. Peralta, A. Melatos, M. Giacobello, and A. Ooi, *Astrophys. J.* **644**, 53 (2006).
- [43] P. D. Lasky, *Publications of the Astronomical Society of Australia* **32**, e034 (2015).
- [44] M. Golubitsky and I. Stewart, *The symmetry perspective: From equilibrium to chaos in phase space and physical space.* (Birkhäuser, Basel, 2003).
- [45] D. Rand, *Arch. Ration. Mech. An.* **79**, 1 (1982).
- [46] M. Golubitsky, V. G. LeBlanc, and I. Melbourne, *J. Nonlinear Sci.* **10**, 69 (2000).
- [47] F. Garcia and F. Stefani, *Proc. Roy. Soc. Lond. A* **474**, 20180281 (2018).
- [48] F. Garcia, M. Seilmayer, A. Giesecke, and F. Stefani, *J. Nonlinear Sci.* **29**, 2735 (2019).
- [49] Y. Plevachuk, V. Sklyarchuk, S. Eckert, G. Gerbeth, and R. Novakovic, *J. Chem. Eng. Data* **59**, 757 (2014).
- [50] E. Doedel and L. S. Tuckerman, eds., *Numerical Methods for Bifurcation Problems and Large-Scale Dynamical Systems*, IMA Volumes in Mathematics and its Applications, Vol. 119 (Springer-Verlag, Berlin, 2000).
- [51] H. A. Dijkstra, F. W. Wubs, A. K. Cliffe, E. Doedel, I. F. Dragomirescu, B. Eckhardt, A. Y. Gelfat, A. L. Hazel, V. Lucarini, A. G. Salinger, E. T. Phipps, J. Sánchez-Umbría, H. Schuttelaars, L. S. Tuckerman, and U. Thiele, *Commun. Comput. Phys.* **15**, 1 (2014).
- [52] J. Sánchez and M. Net, *Eur. Phys. J. Spec. Top.* **225**, 2465 (2016).
- [53] J. Laskar, C. Froeschlé, and A. Celletti, *Physica D* **56**, 253 (1992).
- [54] J. Laskar, *Physica D* **67**, 257 (1993).
- [55] C. K. Mamun and L. S. Tuckerman, *Phys. Fluids* **7**, 80 (1995).
- [56] P. Wulf, C. Egbers, and H. J. Rath, *Phys. Fluids* **11**, 1359 (1999).
- [57] C. Gissinger, H. Ji, and J. Goodman, *Phys. Rev. E* **84**, 026308 (2011).
- [58] J. Wicht and P. Olson, in *Geophysical Research Abstracts* (EGU General Assembly, 2010) p. 10179.
- [59] A differentially rotating flow, for example, provides a natural explanation for the strong axisymmetric character of Saturn's magnetic field [58]